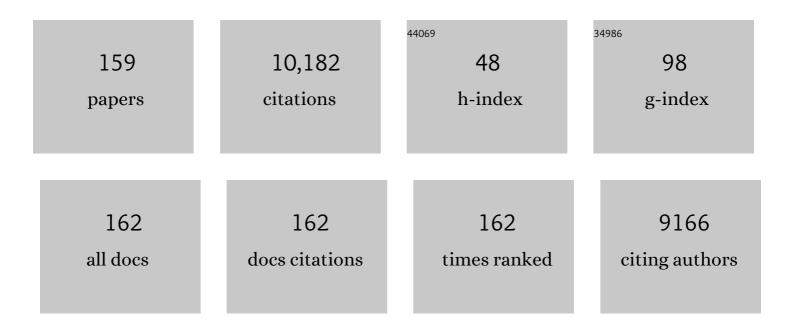
List of Publications by Year in descending order

Source: https://exaly.com/author-pdf/9482426/publications.pdf Version: 2024-02-01



#	Article	IF	CITATIONS
1	MR and fluorescence imaging of gadobutrolâ€induced optical clearing of red fluorescent protein signal in an in vivo cancer model. NMR in Biomedicine, 2022, 35, e4708.	2.8	5
2	In situ decellularization of a large animal saccular aneurysm model: sustained inflammation and active aneurysm wall remodeling. Journal of NeuroInterventional Surgery, 2021, 13, 267-271.	3.3	5
3	Optical clearing and multimodality fluorescence and magnetic resonance imaging in cancer models. , 2021, , .		0
4	Multimodal Bone Metastasis-associated Epidermal Growth Factor Receptor Imaging in an Orthotopic Rat Model. Radiology Imaging Cancer, 2021, 3, e200069.	1.6	1
5	Imaging NFâ€₽̂B activity in a murine model of early stage diabetes. FASEB Journal, 2020, 34, 1198-1210.	0.5	4
6	Synthesis and applications of theranostic oligonucleotides carrying multiple fluorine atoms. Theranostics, 2020, 10, 1391-1414.	10.0	6
7	Magnetic resonance contrast agents in optical clearing: Prospects for multimodal tissue imaging. Journal of Biophotonics, 2020, 13, e201960249.	2.3	21
8	Towards registration of optical and MR signal changes in subcutaneous tumor volume in vivo after optical skin clearing. , 2020, , .		2
9	Optical clearing effects in subcutaneous red-fluorescent tumors monitored by fluorescence and magnetic resonance imaging in vivo (Conference Presentation). , 2020, , .		1
10	Peroxidase Sensitive Amplifiable Probe for Molecular Magnetic Resonance Imaging of Pulmonary Inflammation. ACS Sensors, 2019, 4, 2412-2419.	7.8	17
11	Sensors for Proteolytic Activity Visualization and Their Application in Animal Models of Human Diseases. Biochemistry (Moscow), 2019, 84, 1-18.	1.5	2
12	Antiretroviral Hydrophobic Core Graft-Copolymer Nanoparticles: The Effectiveness against Mutant HIV-1 Strains and in Vivo Distribution after Topical Application. Pharmaceutical Research, 2019, 36, 73.	3.5	5
13	¹⁹ F MRI of Polymer Nanogels Aided by Improved Segmental Mobility of Embedded Fluorine Moieties. Biomacromolecules, 2019, 20, 790-800.	5.4	33
14	Near-infrared oligonucleotide duplex sensors for imaging rapidly activated transcription factors in vitro and in situ. , 2019, , .		0
15	Pilot study to assess visualization and therapy of inflammatory mechanisms after vessel reopening in a mouse stroke model. Scientific Reports, 2018, 8, 745.	3.3	7
16	Dual radiosensitization and anti-STAT3 anti-proliferative strategy based on delivery of gold nanoparticle - oligonucleotide nanoconstructs to head and neck cancer cells Nanotheranostics, 2018, 2, 1-11.	5.2	23
17	High-resolution Imaging of Myeloperoxidase Activity Sensors in Human Cerebrovascular Disease. Scientific Reports, 2018, 8, 7687.	3.3	23
18	Fluorocarbons Enhance Intracellular Delivery of Short STAT3-sensors and Enable Specific Imaging. Theranostics, 2017, 7, 3354-3368.	10.0	12

#	Article	IF	CITATIONS
19	Hydrophobic-core PEGylated graft copolymer-stabilized nanoparticles composed of insoluble non-nucleoside reverse transcriptase inhibitors exhibit strong anti-HIV activity. Nanomedicine: Nanotechnology, Biology, and Medicine, 2016, 12, 2405-2413.	3.3	7
20	Substrate-Based Near-Infrared Imaging Sensors Enable Fluorescence Lifetime Contrast via Built-in Dynamic Fluorescence Quenching Elements. ACS Sensors, 2016, 1, 427-436.	7.8	8
21	Synthesis and Testing of Modular Dual-Modality Nanoparticles for Magnetic Resonance and Multispectral Photoacoustic Imaging. Bioconjugate Chemistry, 2016, 27, 383-390.	3.6	15
22	MR Imaging of Myeloperoxidase Activity in a Model of the Inflamed Aneurysm Wall. American Journal of Neuroradiology, 2015, 36, 146-152.	2.4	13
23	Imaging Inflammation in Cerebrovascular Disease. Stroke, 2015, 46, 2991-2997.	2.0	26
24	Gold Nanoparticles Stabilized with MPEC-Grafted Poly(<scp>l</scp> -lysine): in Vitro and in Vivo Evaluation of a Potential Theranostic Agent. Bioconjugate Chemistry, 2015, 26, 39-50.	3.6	50
25	Aneurysm permeability following coil embolization: packing density and coil distribution. Journal of NeuroInterventional Surgery, 2015, 7, 676-681.	3.3	25
26	Liposomeâ€encapsulated superoxide dismutase mimetic: theranostic potential of an MR detectable and neuroprotective agent. Contrast Media and Molecular Imaging, 2014, 9, 221-228.	0.8	11
27	Myeloperoxidase in Human Intracranial Aneurysms. Stroke, 2014, 45, 1474-1477.	2.0	51
28	Human adipose–derived mesenchymal stem cells attenuate liver ischemia–reperfusion injury and promote liver regeneration. Surgery, 2014, 156, 1225-1231.	1.9	44
29	Superparamagnetic Iron Oxides as Imaging Probes of Metastases and Vulnerable Atherosclerotic Plaques. Frontiers in Nanobiomedical Research, 2014, , 15-45.	0.1	0
30	Protected Graft Copolymer Excipient Leads to a Higher Acute Maximum Tolerated Dose and Extends Residence Time of Vasoactive Intestinal Peptide Significantly Better than Sterically Stabilized Micelles. Pharmaceutical Research, 2013, 30, 670-682.	3.5	3
31	MR Signal Amplification for Imaging of the Mutant EGF Receptor in Orthotopic Human Glioma Model. Molecular Imaging and Biology, 2013, 15, 675-684.	2.6	1
32	The three-dimensional context of a double helix determines the fluorescence of the internucleoside-tethered pair of fluorophores. Molecular BioSystems, 2013, 9, 2447.	2.9	5
33	Fluorescent Macromolecular Sensors of Enzymatic Activity for In Vivo Imaging. Progress in Molecular Biology and Translational Science, 2013, 113, 349-387.	1.7	6
34	Dynamic monitoring of blood–brain barrier integrity using water exchange index (WEI) during mannitol and CO ₂ challenges in mouse brain. NMR in Biomedicine, 2013, 26, 376-385.	2.8	7
35	Modeling Unstable Brain Aneurysms: MR Molecular Imaging of Myeloperoxidase in Vascular Wall and Correlation With Human Pathology. , 2013, , .		0
36	In vivo fluorescence lifetime detection of an activatable probe in infarcted myocardium. Journal of Biomedical Optics, 2012, 17, 056001.	2.6	23

#	Article	IF	CITATIONS
37	A Novel Paramagnetic Substrate for Detecting Myeloperoxidase Activity in Vivo. Molecular Imaging, 2012, 11, 7290.2012.00006.	1.4	6
38	Protected Graft Copolymer (PGC) in Imaging and Therapy: A Platform for the Delivery of Covalently and Non-Covalently Bound Drugs. Theranostics, 2012, 2, 553-576.	10.0	25
39	Sensing of transcription factor binding via cyanine dye pair fluorescence lifetime changes. Molecular BioSystems, 2012, 8, 2166.	2.9	8
40	Protected Graft Copolymer (PGC) Basal Formulation of Insulin as Potentially Safer Alternative to Lantus® (Insulin-Glargine): A Streptozotocin-Induced, Diabetic Sprague Dawley Rats Study. Pharmaceutical Research, 2012, 29, 1033-1039.	3.5	8
41	Orthotopic Expression of Noggin Protein in Cancer Cells Inhibits Human Lung Carcinoma Growth In Vivo. Molecular Imaging and Biology, 2012, 14, 480-488.	2.6	1
42	Tomographic Fluorescence Lifetime Imaging. , 2012, , .		0
43	In Vivo Fluorescence Lifetime Detection of a Cathepsin-Activatable Probe in Infarcted Myocardium. , 2012, , .		0
44	Abstract 2443: MR imaging in human glioma tumor xenograft models using enzyme-conjugated anti-EGFRvIII-specific antibody fragments. , 2012, , .		0
45	A novel paramagnetic substrate for detecting myeloperoxidase activity in vivo. Molecular Imaging, 2012, 11, 433-43.	1.4	4
46	Hairpin-Like Fluorescent Probe for Imaging of NF-κB Transcription Factor Activity. Bioconjugate Chemistry, 2011, 22, 759-765.	3.6	13
47	Molecular Magnetic Resonance Contrast Agents for the Detection of Cancer: Past and Present. Seminars in Oncology, 2011, 38, 42-54.	2.2	39
48	Imaging the pancreatic vasculature in diabetes models. Diabetes/Metabolism Research and Reviews, 2011, 27, 767-772.	4.0	13
49	Targeted Signal-Amplifying Enzymes Enhance MRI of EGFR Expression in an Orthotopic Model of Human Glioma. Cancer Research, 2011, 71, 2230-2239.	0.9	17
50	In vitro and In vivo imaging of antivasculogenesis induced by Noggin protein expression in human venous endothelial cells. FASEB Journal, 2009, 23, 4126-4134.	0.5	10
51	Enzyme-Sensitive Magnetic Resonance Imaging Targeting Myeloperoxidase Identifies Active Inflammation in Experimental Rabbit Atherosclerotic Plaques. Circulation, 2009, 120, 592-599.	1.6	151
52	Plate Capture Assay of Fluorescent Oligonucleotide Duplex Reporterâ~'Transcription Factor Complexes. Bioconjugate Chemistry, 2009, 20, 1444-1448.	3.6	2
53	Carotid Artery Brain Aneurysm Model: In Vivo Molecular Enzyme-specific MR Imaging of Active Inflammation in a Pilot Study. Radiology, 2009, 252, 696-703.	7.3	55
54	Targeted Enzyme-Specific Molecular MR Imaging of Focal Catheter-Induced Vacscular Injury. , 2009, , .		0

#	Article	IF	CITATIONS
55	Validation of Di-5-HT-Gd-DTPA, an Enzyme-Specific MR Contrast Agent for Myeloperoxidase, in the Rabbit Elastase Model of Cerebrovascular Aneurysm. , 2009, , .		0
56	In vivo quantification of transvascular water exchange during the acute phase of permanent stroke. Magnetic Resonance in Medicine, 2008, 60, 813-821.	3.0	29
57	Merging molecular imaging and RNA interference: Early experience in live animals. Journal of Cellular Biochemistry, 2008, 104, 1113-1123.	2.6	17
58	Near-Infrared Fluorescent Oligodeoxyribonucleotide Reporters for Sensing NF-κB DNA Interactions <i>In Vitro</i> . Oligonucleotides, 2008, 18, 235-243.	2.7	14
59	A Novel Thymidine Phosphoramidite Synthon for Incorporation of Internucleoside Phosphate Linkers During Automated Oligodeoxynucleotide Synthesis. Nucleosides, Nucleotides and Nucleic Acids, 2008, 27, 157-172.	1.1	10
60	Fluorescence resonance energy transfer in near-infrared fluorescent oligonucleotide probes for detecting protein–DNA interactions. Proceedings of the National Academy of Sciences of the United States of America, 2008, 105, 4156-4161.	7.1	61
61	Environment-sensitive and Enzyme-sensitive MR Contrast Agents. Handbook of Experimental Pharmacology, 2008, , 37-57.	1.8	10
62	Magnetic Resonance Detection of Inflammation in Elastase-Induced Aneurysms. , 2008, , .		0
63	Noninvasive Magnetic Resonance Imaging of Microvascular Changes in Type 1 Diabetes. Diabetes, 2007, 56, 2677-2682.	0.6	50
64	Cell death in NF-κB-dependent tumour cell lines as a result of NF-κB trapping by linker-modified hairpin decoy oligonucleotide. FEBS Letters, 2007, 581, 1143-1150.	2.8	13
65	Synthesis and Testing of a Binary Catalytic System for Imaging of Signal Amplificationin Vivo. Bioconjugate Chemistry, 2007, 18, 1123-1130.	3.6	16
66	A Paramagnetic Contrast Agent for Detecting Tyrosinase Activity. ChemBioChem, 2007, 8, 1637-1641.	2.6	23
67	Optical Imaging of the Adoptive Transfer of Human Endothelial Cells in Mice Using Anti-Human CD31 Monoclonal Antibody. Pharmaceutical Research, 2007, 24, 1186-1192.	3.5	15
68	Linear Polyethyleneimine Grafted to a Hyperbranched Poly(ethylene glycol)-like Core:Â A Copolymer for Gene Delivery. Bioconjugate Chemistry, 2006, 17, 125-131.	3.6	49
69	A paramagnetic contrast agent with myeloperoxidase-sensing properties. Organic and Biomolecular Chemistry, 2006, 4, 1887.	2.8	58
70	Imaging Molecular Expression on Vascular Endothelial Cells by In Vivo Immunofluorescence Microscopy. Molecular Imaging, 2006, 5, 7290.2006.00004.	1.4	31
71	Targeted imaging of human endothelial-specific marker in a model of adoptive cell transfer. Laboratory Investigation, 2006, 86, 599-609.	3.7	63
72	Amplification strategies in MR imaging: Activation and accumulation of sensing contrast agents (SCAs). Journal of Magnetic Resonance Imaging, 2006, 24, 971-982.	3.4	41

#	Article	IF	CITATIONS
73	Characterizing Vascular Parameters in Hypoxic Regions: A Combined Magnetic Resonance and Optical Imaging Study of a Human Prostate Cancer Model. Cancer Research, 2006, 66, 9929-9936.	0.9	65
74	Imaging of Myeloperoxidase in Mice by Using Novel Amplifiable Paramagnetic Substrates. Radiology, 2006, 240, 473-481.	7.3	147
75	Imaging molecular expression on vascular endothelial cells by in vivo immunofluorescence microscopy. Molecular Imaging, 2006, 5, 31-40.	1.4	18
76	Myeloperoxidase Activity Imaging Using 67Ga Labeled Substrate. Molecular Imaging and Biology, 2005, 7, 403-410.	2.6	17
77	Detection of Early Antiangiogenic Effects in Human Colon Adenocarcinoma Xenografts: In vivo Changes of Tumor Blood Volume in Response to Experimental VEGFR Tyrosine Kinase Inhibitor. Cancer Research, 2005, 65, 9253-9260.	0.9	26
78	DTPA-bisamide-Based MR Sensor Agents for Peroxidase Imaging. Organic Letters, 2005, 7, 1719-1722.	4.6	101
79	Imaging of VEGF Receptor Kinase Inhibitor-Induced Antiangiogenic Effects in Drug-Resistant Human Adenocarcinoma Model. Neoplasia, 2005, 7, 847-853.	5.3	34
80	Methotrexate-Induced Accumulation of Fluorescent Annexin V in Collagen-Induced Arthritis. Molecular Imaging, 2005, 4, 153535002005041.	1.4	22
81	Visualization of antitumor treatment by means of fluorescence molecular tomography with an annexin V-Cy5.5 conjugate. Proceedings of the National Academy of Sciences of the United States of America, 2004, 101, 12294-12299.	7.1	355
82	Measurement of tumor interstitial volume fraction: Method and implication for drug delivery. Magnetic Resonance in Medicine, 2004, 52, 485-494.	3.0	34
83	Human myeloperoxidase: A potential target for molecular MR imaging in atherosclerosis. Magnetic Resonance in Medicine, 2004, 52, 1021-1028.	3.0	127
84	Novel Hyperbranched Dendron for Gene Transfer in Vitro and in Vivo. Bioconjugate Chemistry, 2004, 15, 960-968.	3.6	42
85	Synthesis and Properties of Fluorescent NF-κB-Recognizing Hairpin Oligodeoxyribonucleotide Decoys. Bioconjugate Chemistry, 2004, 15, 1481-1487.	3.6	15
86	Engineering of technetium-99m-binding artificial receptors for imaging gene expression. Journal of Gene Medicine, 2003, 5, 1056-1066.	2.8	23
87	Optical Imaging of Apoptosis as a Biomarker of Tumor Response to Chemotherapy. Neoplasia, 2003, 5, 187-192.	5.3	111
88	Near-infrared fluorescent imaging of tumor apoptosis. Cancer Research, 2003, 63, 1936-42.	0.9	164
89	In vivo imaging in the development of gene therapy vectors. Current Opinion in Molecular Therapeutics, 2003, 5, 594-602.	2.8	5
90	Steady-state and Dynamic Contrast MR Imaging of Human Prostate Cancer Xenograft Tumors: A Comparative Study. Technology in Cancer Research and Treatment, 2002, 1, 489-495.	1.9	12

#	Article	lF	CITATIONS
91	Imaging of Differential Protease Expression in Breast Cancers for Detection of Aggressive Tumor Phenotypes. Radiology, 2002, 222, 814-818.	7.3	161
92	Magnetic Resonance Imaging of Inducible E-Selectin Expression in Human Endothelial Cell Culture. Bioconjugate Chemistry, 2002, 13, 122-127.	3.6	215
93	Cellular Activation of the Self-Quenched Fluorescent Reporter Probe in Tumor Microenvironment. Neoplasia, 2002, 4, 228-236.	5.3	56
94	Viral imaging in gene therapy. Neuroimaging Clinics of North America, 2002, 12, 571-581.	1.0	8
95	Oligomerization of Paramagnetic Substrates Result in Signal Amplification and Can be Used for MR Imaging of Molecular Targets. Molecular Imaging, 2002, 1, 153535002002000.	1.4	21
96	In vivo imaging of gene delivery and expression. Trends in Biotechnology, 2002, 20, S11-S18.	9.3	52
97	Targeting of MPEG-protected polyamino acid carrier to human E-selectin in vitro. Amino Acids, 2002, 23, 301-308.	2.7	19
98	Annexin V–CLIO: A Nanoparticle for Detecting Apoptosis by MRI. Molecular Imaging, 2002, 1, 153535002002021.	1.4	54
99	Annexin V—CLIO: A Nanoparticle for Detecting Apoptosis by MRI. Molecular Imaging, 2002, 1, 102-107.	1.4	148
100	Oligomerization of Paramagnetic Substrates Result in Signal Amplification and can be Used for MR Imaging of Molecular Targets. Molecular Imaging, 2002, 1, 16-23.	1.4	126
101	Size Optimization of Synthetic Graft Copolymers for in Vivo Angiogenesis Imaging. Bioconjugate Chemistry, 2001, 12, 213-219.	3.6	79
102	DNA binding chelates for nonviral gene delivery imaging. Gene Therapy, 2001, 8, 515-522.	4.5	20
103	New approaches for imaging in gene therapy. European Journal of Radiology, 2000, 34, 156-165.	2.6	52
104	Tumoral Distribution of Long-circulating Dextran-coated Iron Oxide Nanoparticles in a Rodent Model. Radiology, 2000, 214, 568-574.	7.3	357
105	In vivo imaging of tumors with protease-activated near-infrared fluorescent probes. Nature Biotechnology, 1999, 17, 375-378.	17.5	1,578
106	Approaches and agents for imaging the vascular system. Advanced Drug Delivery Reviews, 1999, 37, 279-293.	13.7	48
107	Mechanism of gadophrin-2 accumulation in tumor necrosis. Journal of Magnetic Resonance Imaging, 1999, 9, 336-341.	3.4	52

108 In vivo assessment of vascular endothelial growth factor-induced angiogenesis. , 1999, 83, 798-802.

46

#	Article	IF	CITATIONS
109	Near-Infrared Optical Imaging of Protease Activity for Tumor Detection. Radiology, 1999, 213, 866-870.	7.3	571
110	Targeting of Green Fluorescent Protein Expression to the Cell Surface. Biochemical and Biophysical Research Communications, 1999, 262, 638-642.	2.1	19
111	Cerebrovascular Dynamics of Autoregulation and Hypoperfusion. Stroke, 1999, 30, 2197-2205.	2.0	138
112	Design of metal-binding green fluorescent protein variants. Biochimica Et Biophysica Acta Gene Regulatory Mechanisms, 1998, 1397, 56-64.	2.4	23
113	The development of in vivo imaging systems to study gene expression. Trends in Biotechnology, 1998, 16, 5-10.	9.3	85
114	Continuous assessment of perfusion by tagging including volume and water extraction (CAPTIVE): A steady-state contrast agent technique for measuring blood flow, relative blood volume fraction, and the water extraction fraction. Magnetic Resonance in Medicine, 1998, 40, 666-678.	3.0	51
115	Non-invasive in vivo mapping of tumour vascular and interstitial volume fractions. European Journal of Cancer, 1998, 34, 1448-1454.	2.8	50
116	Antibody-Mediated versus Nontargeted Delivery in a Human Small Cell Lung Carcinoma Model. Bioconjugate Chemistry, 1998, 9, 184-191.	3.6	48
117	Novel Gliosarcoma Cell Line Expressing Green Fluorescent Protein: A Model for Quantitative Assessment of Angiogenesis. Microvascular Research, 1998, 56, 145-153.	2.5	45
118	Preclinical evaluation and phase I clinical trial of a 99mTc-labeled synthetic polymer used in blood pool imaging American Journal of Roentgenology, 1998, 171, 137-143.	2.2	46
119	MR imaging of gene delivery to the central nervous system with an artificial vector Radiology, 1998, 208, 65-71.	7.3	32
120	Mapping the <i>In Vivo</i> Distribution of Herpes Simplex Virions. Human Gene Therapy, 1998, 9, 1543-1549.	2.7	63
121	MR imaging and scintigraphy of gene expression through melanin induction Radiology, 1997, 204, 425-429.	7.3	198
122	A Long-Circulating co-Polymer in "Passive Targeting―to Solid Tumors. Journal of Drug Targeting, 1997, 4, 321-330.	4.4	69
123	In Vivo localization of diglycylcysteine-bearing synthetic peptides by nuclear imaging of oxotechnetate transchelation. Nuclear Medicine and Biology, 1997, 24, 739-742.	0.6	15
124	Magnetically labeled cells can be detected by MR imaging. Journal of Magnetic Resonance Imaging, 1997, 7, 258-263.	3.4	336
125	Uptake of dextran-coated monocrystalline iron oxides in tumor cells and macrophages. Journal of Magnetic Resonance Imaging, 1997, 7, 1140-1145.	3.4	266
126	Relative Blood Volume Measurements by Magnetic Resonance Imaging Facilitate Detection of Testicular Torsion. Investigative Radiology, 1997, 32, 763-769.	6.2	11

#	Article	IF	CITATIONS
127	Magnetically Labeled Secretin Retains Receptor Affinity to Pancreas Acinar Cells. Bioconjugate Chemistry, 1996, 7, 311-316.	3.6	50
128	An Adduct ofcis-Diamminedichloroplatinum(II) and Poly(ethylene glycol)poly(l-lysine)â^'Succinate:Â Synthesis and Cytotoxic Properties. Bioconjugate Chemistry, 1996, 7, 144-149.	3.6	50
129	Improving MR quantification of regional blood volume with intravascularT1 contrast agents: Accuracy, precision, and water exchange. Magnetic Resonance in Medicine, 1996, 36, 858-867.	3.0	153
130	Long-circulating iron oxides for MR imaging. Advanced Drug Delivery Reviews, 1995, 16, 321-334.	13.7	374
131	Long-circulating blood pool imaging agents. Advanced Drug Delivery Reviews, 1995, 16, 335-348.	13.7	56
132	Quantitation of slow drug release from an implantable and degradable gentamicin conjugate by in vivo magnetic resonance imaging. Antimicrobial Agents and Chemotherapy, 1995, 39, 839-845.	3.2	20
133	Experimental gastrointestinal hemorrhage: detection with contrast-enhanced MR imaging and scintigraphy Radiology, 1995, 196, 239-244.	7.3	20
134	Inflammation: imaging with methoxy poly(ethylene glycol)-poly-L-lysine-DTPA, a long-circulating graft copolymer Radiology, 1995, 197, 665-669.	7.3	19
135	Determinants of in vivo MR imaging of slow axonal transport Radiology, 1994, 193, 485-491.	7.3	33
136	Detection of pulmonary emboli by using MR angiography with MPEG-PL-GdDTPA: an experimental study in rabbits American Journal of Roentgenology, 1994, 162, 1041-1046.	2.2	32
137	Targeted delivery of diagnostic agents by surface-modified liposomes. Journal of Controlled Release, 1994, 28, 45-58.	9.9	52
138	Intravenous carriers for drug delivery to lymph nodes. Journal of Controlled Release, 1994, 28, 293-294.	9.9	3
139	Macromolecular complexone for detection of microvasculature by magnetic resonance angiography. Journal of Controlled Release, 1994, 28, 325-326.	9.9	0
140	Liposomal diamidine (imidocarb): Preparation and animal studies. Journal of Microencapsulation, 1994, 11, 627-632.	2.8	11
141	Poly(ethylene glycol) on the liposome surface: on the mechanism of polymer-coated liposome longevity. Biochimica Et Biophysica Acta - Biomembranes, 1994, 1195, 11-20.	2.6	419
142	Trapping of dextran-coated colloids in liposomes by transient binding to aminophospholipid: preparation of ferrosomes. Biochimica Et Biophysica Acta - Biomembranes, 1994, 1193, 212-218.	2.6	61
143	MR lymphography: study of a high-efficiency lymphotrophic agent Radiology, 1994, 191, 225-230.	7.3	122
144	Monocrystalline iron oxide nanocompounds (MION): Physicochemical properties. Magnetic Resonance in Medicine, 1993, 29, 599-604.	3.0	511

#	Article	IF	CITATIONS
145	Polymeric contrast agents for MR imaging of adrenal glands. Journal of Magnetic Resonance Imaging, 1993, 3, 93-97.	3.4	10
146	Colloidal magnetic resonance contrast agents: effect of particle surface on biodistribution. Journal of Magnetism and Magnetic Materials, 1993, 122, 383-386.	2.3	116
147	Mion-ASF: Biokinetics of an MR receptor agent. Magnetic Resonance Imaging, 1993, 11, 411-417.	1.8	61
148	MR Imaging of Slow Axonal Transport in Vivo. Experimental Neurology, 1993, 123, 235-242.	4.1	25
149	Asymmetry in <i>trans</i> -bilayer lateral pressure may drive expansion of the secretion fusion pore. Biochemical Society Transactions, 1993, 21, 271-275.	3.4	13
150	A Drug System (PDH) for Interventional Radiology Synthesis, Properties, and Efficacy. Investigative Radiology, 1993, 28, 1083-1089.	6.2	4
151	Destabilization of pH-sensitive liposomes in the presence of human erythrocyte ghosts. Journal of Controlled Release, 1992, 20, 219-229.	9.9	17
152	The fusion of artificial lipid membranes induced by the synthetic arenavirus â€~fusion peptide'. Biochimica Et Biophysica Acta - Biomembranes, 1992, 1110, 202-208.	2.6	31
153	Restoration of adhesive potentials of Ehrlich ascites carcinoma cells by modification of plasma membrane. Journal of Cellular Physiology, 1991, 147, 182-190.	4.1	12
154	Lectin-bearing liposomes: Differential binding to normal and to transformed mouse fibroblasts. Experimental Cell Research, 1989, 181, 362-374.	2.6	16
155	Biotin-Bearing pH-Sensitive Liposomes: High-Affinity Binding to Avidin Layer. Journal of Liposome Research, 1989, 1, 233-244.	3.3	4
156	Protein immobilization on the surface of liposomes via carbodiimide activation in the presence of N-hydroxysulfosuccinimide. FEBS Letters, 1988, 231, 381-384.	2.8	65
157	Adhesion defect of ascites cells corrected with membrane-bound attachment molecules. FEBS Letters, 1988, 241, 185-187.	2.8	1
158	Thiolation of preformed liposomes with iminothiolane. FEBS Letters, 1987, 214, 13-16.	2.8	8
159	Protein Immobilization on Liposomes. Annals of the New York Academy of Sciences, 1984, 434, 580-581.	3.8	2